Published in final edited form as:
Chem Biol Interact. 2009 March 16; 178(1-3): 16–23. doi:10.1016/j.cbi.2008.10.037.

Activity of Yeast Alcohol Dehydrogenases on Benzyl Alcohols and Benzaldehydes. Characterization of ADH1 from *Saccharomyces carlsbergensis* and Transition State Analysis

Suresh Pal, **Doo-Hong Park**, and **Bryce V. Plapp***
Department of Biochemistry, The University of Iowa, Iowa City, Iowa 52242-1109 USA

Abstract

The substrate specificities of yeast alcohol dehydrogenases I and II from *Saccharomyces cerevisiae* (*Sce*ADH1 and *Sce*ADH2) and *Saccharomyces carlsbergensis* (*Scb*ADH1) were studied. For this work, the gene for the *S. carlsbergensis* ADH1 was cloned, sequenced and expressed. The amino acid sequence of *Scb*ADH1 differs at four positions as compared to *Sce*ADH1, including substitutions of two glutamine residues with glutamic acid residues, and has the same sequence as the commercial yeast enzyme, which apparently is prepared from *S. carlsbergensis*. The electrophoretic mobilities of *Scb*ADH1, *Sce*ADH2 and commercial ADH are similar. The kinetics and specificities of *Scb*ADH1 and *Sce*ADH1 acting on branched, long-chain and benzyl alcohols are very similar, but the catalytic efficiency of *Sce*ADH2 is about 10 to 100-fold higher on these substrates. A three dimensional structure of *Sce*ADH1 shows that the substrate binding pocket has Met-270, whereas *Sce*ADH2 has Leu-270, which allows larger substrates to bind. The reduction of a series of *p*-substituted benzaldehydes catalyzed by *Sce*ADH2 is significantly enhanced by electron-withdrawing groups, whereas the oxidation of *p*-substituted aromatic alcohols may be only slightly affected by the substituents. The substituent effects on catalysis generally reflect the effects on the equilibrium constant for the reaction, where electron-withdrawing substituents favor alcohol. The results are consistent with a transition state that is electronically similar to the alcohol, supporting previous results obtained with commercial yeast ADH.

Keywords

Alcohol dehydrogenase; Substrate specificity; Enzyme kinetics; Quantitative structure-activity relationships; Transition state; X-ray crystallography

1. Introduction

The zinc-containing, medium-chain alcohol dehydrogenases catalyze the interconversion of ethanol and NAD^+ to acetaldehyde and NADH, and they are commonly found in bacteria, yeasts, plants and animals [1–3]. Mammalian ADHs react efficiently with a great variety of alcohols, aldehydes, and ketones, but yeast ADHs have more restricted specificities and are most active on ethanol and acetaldehyde [4,5]. The yeast *S. cerevisiae* produces three ADH isoenzymes - ADH1, ADH2, and ADH3. ADH1 is the constitutive, cytoplasmic form that

*Corresponding author. Tel.:+1-319-335-7909; fax 319-335-9570. E-mail: E-mail: bv-plapp@uiowa.edu).

reduces acetaldehyde during fermentation of glucose [6–8]. A three-dimensional structure of this enzyme has been determined (2HCY.pdb). ADH2 is also a cytoplasmic form, but it is repressed by glucose and functions to oxidize ethanol in aerobic metabolism [9]. ADH3 is a mitochondrial form, perhaps involved as a shuttle for reducing equivalents in NADH [10]. The kinetic constants of the *S. cerevisiae* enzymes are similar, except that ADH2 has about a 20-fold lower K_m and 10-fold higher catalytic efficiency (V_1/K_m) for ethanol [11].

The mechanism of hydrogen transfer catalyzed by yeast ADH was studied extensively in a series of significant papers, using substituted benzyl alcohols and benzaldehydes [12–16]. However, the studies led to conflicting conclusions about the structure of the transition state. Quantitative structure-activity relationship studies with *p*-substituted benzyl alcohols and aldehydes suggested that the transition state resembled alcohol with little or no charge development at C-7 [14]. In contrast, the α-secondary k_H/k_T isotope effects for oxidation of benzyl alcohols were within error the same as the equilibrium isotope effects, suggesting that the transition state resembles aldehyde [15]. Further studies of the isotope effects suggested that hydride is transferred with quantum mechanical tunneling, with coupled motion and a transition state similar to alcohol [16]. The commercial enzyme used for these studies has much less activity on the aromatic substrates than on ethanol or acetaldehyde, but the cloned isoenzyme I from *S. cerevisiae* (*Sce*ADH1) had “no detectable activity” on benzyl alcohol, *i.e.*, less than $1/10^5$ of the activity on ethanol [4]. Thus, the origin of the activity on benzyl alcohol is uncertain, and we sought to determine which ADHs are active on benzyl alcohol and benzaldehyde.

The protein sequence of commercial yeast ADH is microheterogeneous [6], and it was suggested that the preparations contain ADH1 and ADH2 [17]. We noted that commercial preparations of yeast ADH are electrophoretically heterogeneous, with major components migrating with mobilities similar to that of the major enzyme isolated from *S. carlsbergensis*, brewer’s yeast, and to *Sce*ADH2, but different than *Sce*ADH1. *S. cerevisiae* is a top fermenting yeast for brewing ales, and *S. calsbergensis* is a bottom fermenting yeast for brewing lager beers [18]. These are related species [19], but *S. carlsbergensis* is also named *S. pastorianus* and may be a hybrid between *S. cerevisiae* and *S. monacensis* [20] or between *S. cerevisiae* and *S. bayanus* [21]. We cloned and expressed the gene for ADH1 from *S. carlsbergensis* and compared its activities on various substrates with the activities of SceADH1 and SceADH2. *Sce*ADH2 was identified as the isoenzyme most active on the aromatic substrates, and it was used to repeat the studies on the *p*-substituted benzyl alcohols and benzaldehydes.

2. Experimental Procedures

2.1. Materials

All alcohols were obtained from Aldrich or Fisher Scientific and redistilled before use. DEAE-Sepharose CL-4B and Octyl-Sepharose CL-4B were purchased from Pharmacia P-L Biochemicals. $LiNAD^+$ and Na_2NADH were the best grades available from Boehringer Mannheim, and pyrazole was purchased from Eastman Kodak. Commercial yeast ADH was obtained from Boehringer Mannheim Corporation, Cooper Labs, or Sigma Chemical Co.

2.2. Cloning and Expression

Genomic DNA was isolated from *S. carlsbergensis* strain Y379-50 by standard procedures [22]. DNA fragments of about 1600 base-pairs produced by restriction enzyme *Sph*I were identified by hybridization with the *ADH1* gene from *S. cerevisiae* and subcloned into the yeast expression plasmid YEp13, which was transformed into *E. coli* strain DH5α [23]. Colonies containing the *ADH* gene were identified by hybridization with the *SceADH1* gene, and the

plasmid was purified and characterized by restriction mapping and DNA sequencing [24]. One strand of the plasmid was sequenced with four different primers, providing the complete sequence for the coding region and 283 nucleotides of the 5′ and 186 nucleotides of the 3′ flanking regions. (The DNA sequence for the *Saccharomyces carlbergensis ADH1* has been deposited in the GenBank/Embl Data Bank with accession number FJ195977.) Yeast strain 302-21#2, which does not produce ADHs [11], was transformed with the plasmid, and cells with the YEp13 plasmid were selected on synthetic medium lacking leucine.

2.3 Enzyme purification and characterization

Yeast transformed with plasmids expressing the *ADH1* and *ADH2* genes from *S. cerevisiae* and the *ADH1* gene from *S. carlsbergensis* were grown in rich media, and the recombinant enzymes were purified as described previously [11,25]. The final enzyme preparations appeared to be at least 90 % pure by polyacrylamide gel electrophoresis in the presence or absence of sodium dodecyl sulfate [26]. Enzyme concentrations were determined by titration of the active sites with NAD^+ in the presence of 10 mM pyrazole [27].

2.4. Enzyme kinetics

Activities on various substrates was determined in 83 mM potassium phosphate, 40 mM KCl, and 0.25 mM EDTA buffer, pH 7.3, at 30 °C, conditions that are similar to those in living yeast. The initial velocities for the change of absorbance at 340 nm on CARY 118C spectrophotometer were estimated by a linear or parabolic fit to the progress curve. Because the enzyme activities on many of the alcohols (other than linear aliphatic alcohols) studied here were relatively low, large amounts of enzyme (up to 0.1 mg/ml) were used. Contamination of solutions by readily oxidized alcohols was minimized by using redistilled alcohols and purified water. Activities were always at least 5 times higher than the activity determined in the absence of added alcohol. For assays with poor substrates, progress curves were obtained for about 5 min, and any small “burst” of activity (due to contaminants) was ignored in the analysis of the initial velocity. As a test of the procedures, *tert*-butyl alcohol was tested as a substrate and “activity” was less than 1/10th of the activity on the poorest substrate. Concentrations of alcohols were used that did not produce substrate inhibition, and the highest concentrations are reported in the results. The kinetic data were fitted to the appropriate equations using the programs HYPER for fitting to the Michaelis-Menten equation when one substrate is varied, SEQUEN or PING PONG for fitting initial velocity data for studies when coenzyme and substrate concentrations were each varied over a 9-fold range for a total of 25 combinations of concentrations, and COMP or NONCOMP for product inhibition studies [28]. The standard errors of the kinetic constants were usually less than 25 % of the values, indicating good precision and fits. In general, the values should be reproducible within a factor of 2.

The products of oxidation of benzyl alcohol in a reaction mixture containing 2 mM NAD^+, 50 mM benzyl alcohol, and 10 to 30 μg/ml of enzyme at pH 7.3 and 30 °C were also determined. The production of NADH was followed at 340 nm. Production of benzaldehyde was determined by HPLC. Aliquots of 200 μl were taken at various times of reaction (up to 90 or 180 min) and immediately quenched in 800 μl of acetonitrile/acetic acid/water (30:1:69) containing 1 mM *p*-bromobenzoic acid as a internal standard. Samples were chromatographed on an Altex Ultrasphere Octyl column (4.6 mm × 25 cm) developed with acetonitrile/acetic acid/water (30:1:69) at 1 ml/min, with detection of the products at 254 nm [29].

3. Results

3.1. Characterization of *S. carlsbergensis* ADH1

As compared to the gene for *Sce*ADH1, the DNA sequence for *Scb*ADH1 differs at 12 positions in the coding region and 2 in the 3′-flanking region. These changes would result in four

substitutions in the amino acid sequence, as listed in Table 1. In three out of these four positions, *Scb*ADH1 has the same amino acid sequence as does *Sce*ADH2 and commercial ADH, thought to be from *S. cerevisiae* [6], but *Sce*ADH1 and *Sce*ADH2 differ at 23 amino acid residues [9]. We conclude that *Scb*ADH1 is the homolog of *Sce*ADH1. The *Scb*ADH1 gene differs at 41 of 1044 nucleotides in the coding region of the *S. pastorianus* ADH1 gene. The sequence of the *Sce*ADH1 gene [8] showed five differences as compared to the protein sequence determined from the commercial enzyme, but preparations of commercial enzyme may be microheterogeneous [17]. Our sequencing of the *Sce*ADH1 gene [11] and X-ray crystallography (2HCY.pdb) gave the same sequence and showed that residue 20 is tyrosine, not histidine. Mass spectrometry of tryptic peptides of high quality commercial yeast ADH confirmed the amino acid compositions predicted from the DNA sequence for *Scb*ADH1 (data not shown). The results show that commercial yeast enzyme apparently is prepared from *S. carlsbergensis*.

The differences in amino acid sequences of the ADHs are also apparent on gel electrophoresis under non-denaturing conditions, at pH 8.4, where enzyme is located by activity or protein stain (Table 2). *Scb*ADH1 migrates faster than *Sce*ADH1, slower than *Sce*ADH3, and at about the same rate as *Sce*ADH2 or commercial enzymes (which are heterogeneous and have a broad band). All enzymes migrate with the same relative molecular weight under denaturing conditions. The increased mobility of *Scb*ADH1 relative to *Sce*ADH1 can be explained by the two additional negative charges due to the glutamates at positions 127 and 147. Electrophoretic mobilities are also altered with site-directed mutations that change one charge [25,30,31]. However, the change in mobility is not simply proportional to the change in charge, and although *Sce*ADH1 and *Sce*ADH2 have the same calculated net charge they migrate differently.

The kinetic constants of *Scb*ADH1 obtained from initial velocity studies are most similar to those for *Sce*ADH1 for the oxidation of ethanol and reduction of acetaldehyde (Table 3). *Scb*ADH1 appears to have about a 2-fold higher turnover number for reduction of acetaldehyde than *Sce*ADH1 does, which might explain the vigorous fermentative ability of *S. carlsbergensis*. *Sce*ADH2 has lower turnover numbers than the ADH1s, but catalytic efficiency is higher because the K_b (Michaelis constant for ethanol) and K_p (Michaelis constant for acetaldehyde) are 7 to 20-fold smaller. The kinetic mechanism for yeast ADHs acting on ethanol and acetaldehyde is predominantly ordered Bi Bi, as shown by previous experiments [11,32,33].

3.2. Substrate Specificities

The kinetic constants describing the activities of these ADHs on various alcohols are compared in Table 4. *Sce*ADH1 and *Scb*ADH1 show about the same specificities, but *Sce*ADH2 has significantly higher activity (V_1/E_t and V_1/K_b) for all of the alcohols. These results again confirm that the cloned *S. carlsbergensis* gene codes for ADH1. The secondary and branched chain alcohols are oxidized with much lower turnover numbers and catalytic efficiencies than the linear, primary alcohols. The variation in turnover numbers is consistent with hydride transfer being rate-limiting for catalysis, as has been confirmed by the significant deuterium isotope effect on V_1/E_t for oxidation of 2-propanol [34,35]. All of these enzymes prefer the *S*-isomer of butanol as compared to the *R*-isomer. Similar results were obtained earlier with commercial yeast ADH [5,36]. In general, increasing the size of the alcohol or introducing branching with additional methyl groups decreases catalytic efficiency for *Sce*ADH1 [4,11]. The yeast enzyme is inactive towards secondary alcohols where both alkyl groups are ethyl or larger [5], and we detected no activity with cyclohexanol as a substrate (although we found it to be a competitive inhibitor against ethanol with a K_i value of 7.8 mM).

In order to determine which yeast ADHs are active on benzyl alcohols and aldehydes, we surveyed the activities of the three isoenzymes. Table 5 shows that the activities (V/K_m) on these aromatic substrates are 3 to 5 orders of magnitude lower than the activities on ethanol and acetaldehyde (Table 3). *Sce*ADH1 and *Scb*ADH1 show similar substrate specificities, but *Sce*ADH2 is about one order of magnitude more active (V/E_t and V/K_m) than *Sce*ADH1 and *Scb*ADH1. The activity of *Sce*ADH1 on benzyl alcohol is about $1/10^5$ of that on ethanol, confirming the previous conclusion [4]. Significantly for these studies, *Sce*ADH2 is about 100 times more active than *Sce*ADH1 is on benzyl alcohol.

Since the rates of oxidation of benzyl alcohol as determined by the change in NADH concentration are so slow, it is important to ascertain that benzyl alcohol is being oxidixed to benzaldehyde. The formation of benzaldehyde from benzyl alcohol upon oxidation with NAD^+ as catalyzed by *Sce*ADH1, *Scb*ADH1 and *Sce*ADH2 was confirmed by HPLC analyses. The concentrations of the products benzaldehyde and NADH were very similar throughout the course of the reaction, indicating a stoichiometric reaction. The rates of the reaction were comparable to those determined by steady-state kinetics. No benzoic acid was detected, suggesting that yeast ADH does not catalyze the dismutation of benzaldehyde, in contrast to the action of horse liver ADH [29].

The activity of a commercial preparation of yeast ADH on benzyl alcohol gave a V_1/E_t of 0.058 s^{-1} and a V_1/K_b of 1.7 $M^{-1}s^{-1}$, which is about 4 times larger than the values obtained for the cloned *Sce*ADH1 or *Scb*ADH1 (compare to Table 5). Since the commercial preparation is electrophoretically heterogeneous, it may contain a mixture of ADH1 and ADH2. Using the kinetic constants (V_1/K_b) for the cloned enzymes, we can estimate that the commercial enzyme has about 3 % ADH2, which would contribute about 75 % of the activity on benzyl alcohol. The percentage may vary with different preparations, of course.

3.3. Quantitative structure-activity relationships

The relationships for the reactions of the *p*-substituted benzyl alcohols and benzaldehydes were studied previously with commercial yeast enzyme [12,14], but it seemed prudent to repeat these studies using a single enzyme form. The kinetic constants for *Sce*ADH2 acting on *p*-substituted aromatic alcohols and aldehydes were determined by varying the concentrations of both coenzyme and substrate and fitting the data to the equation for a sequential bi-substrate reaction, which provides true kinetic constants. As shown in Table 6, the *p*-substitutions have relatively small effects on alcohol oxidation, in particular on V_1/E_t and V_1/K_b, which report on the hydrogen transfer step and the catalytic efficiency, respectively. The kinetic constants are similar to those observed previously [14], except that the turnover numbers are somewhat higher in the present study. It is difficult to compare the values directly because alcohol oxidation is faster at pH above a pK of 8.25 [13], and the previous study was done at pH 8.5 and 25 °C and the present study at pH 7.3 and 30 °C.

For the reduction of the aldehydes, in contrast, the *p*-substituents have large effects, with electron-withdrawing substituents increasing V_2/E_t and V_2/K_p by about 100-fold over the range studied (Table 7). The overall magnitude of the electronic effects on V_2/E_t is very similar to the previous results [12], but the turnover numbers are about 30-fold larger in the present study, in part due to the lower pH used in the present study. The Michaelis constants for the benzaldehydes are similar in magnitude to those in the previous study, but the dependence of V_2/K_p on the electronic effects differs. The internal consistency of the kinetic constants was checked by calculating the Haldane relationship, $K_{eq} = V_1K_pK_{iq}[H^+]/V_2K_bK_{ia}$, which gave reasonably good agreement with the values determined by Klinman [14] for the *p*-CH_3O-, CH_3-, Cl-, and Br- compounds.

The classical approach for analyzing the electronic effects of substituents uses the Hammett equation, supplemented by consideration of the hydrophobicity, molar refractivity, and van der Waals radii of the substituents, which may be factors in determining the enzyme specificity [37,38]. Multiple linear regression of the data for benzyl alcohol oxidation showed no significant correlation of the kinetic constants with any of these factors, because the rate constants were essentially not affected by the substituents. Fig. 1 shows the relationship of V_1/E_t and V_1/K_b. with σ^+, which describes reactions in which electron donation by resonance to the reaction center is important [37]. In contrast, the reduction of the benzaldehydes as measured by V_2/E_t or V_2/K_p showed a good correlation with σ^+ with a ρ value (slope of the dependence) of 1.9 or 1.7 (Fig. 2). The substituent effects on K_p alone are relatively small, as shown by inspection of the data in Table 7 and the similar slopes of the lines in Fig. 2. Combinations with additional factors resulted in modestly better fits, but more data points (additional substituted benzaldehydes) would be required to justify including the other factors.

4. Discussion

4.1. Enzyme structure and substrate specificities

The cloning and sequencing of the *ADH1* gene from *S. carlsbergensis* shows that *Scb*ADH1 differs from *Sce*ADH1 by four amino acid residues, which change the electrophoretic mobility of the proteins, but cause only small effects on the kinetic constants for enzymatic activity on various substrates. It appears that commercial yeast ADH is produced from *S. carlsbergensis* and contains predominantly ADH1. The commercial ADH does not appear to be produced from *S. pastorianus*, which is the name also used for *S. carlsbergensis*. However, commercial ADH preparations are usually heterogeneous and may also contain ADH2. The *ADH2* gene from *S. carlsbergensis* should also be cloned so that *Scb*ADH2 can be characterized. *Sce*ADH2 has an electrophoretic mobility similar to that *Scb*ADH1, but clearly differs by having higher activity (V_1/E_t and V_1/K_m) on aliphatic, branched chain, and aromatic alcohols.

*Sce*ADH2 is more active than *Sce*ADH1 on the larger alcohols. These enzymes differ in 24 amino acid residues (if position 20 is considered), but the only difference in the substrate binding site is Leu-270 in *Sce*ADH2 as compared to Met-270 in *Sce*ADH1 and *Scb*ADH1. *Sce*ADH3 also has Leu-270 [10], and its activity on benzyl alcohol should be determined. The M270L substitution in *Sce*ADH1 increases catalytic efficiency with butanol, pentanol, and hexanol, but not on ethanol or propanol [11]. Residues distant from the active site must be implicated in the 10-fold higher catalytic activity of *Sce*ADH2 as compared to *Sce*ADH1 on ethanol (Table 3), but these have not been identified.

A three-dimensional structure of *Sce*ADH1 complexed with NAD^+ and 2,2,2-trifluoroethanol has been determined by X-ray crystallography (2HCY.pdb), which makes it possible to explain the higher activity of *Sce*ADH2 as compared to *Sce*ADH1 on benzyl alcohol. A model of the yeast enzyme was constructed by replacing the trifluoroethanol with the benzyl alcohol, positioning the hydroxymethyl group so that the *pro-R* hydrogen is directed toward C4 of the nicotinamide ring, and rotating the benzene ring into the position with optimized contacts with the amino acid residues (Fig. 3). *Sce*ADH1 has Thr-45, Trp-54, Trp-92, Met-270 and Tyr-294 in close contact with the substrate, but Met-270 makes a bad contact (1.8 Å) that is not relieved by changing rotamers. The M270L substitution would relieve some of the steric hindrance as illustrated in Fig. 3. Nevertheless, some close contacts remain, and we must assume that the enzymes are somewhat flexible if benzyl alcohol can bind and be oxidized.

Horse liver ADH has a large substrate binding site and readily accommodates and efficiently oxidizes benzyl alcohol, cyclohexanol, and branched chain alcohols [39–41]. The horse enzyme has much higher activity than *Sce*ADH1 does on branched chain alcohols [4]. The lower activity of *Sce*ADH1 with larger alcohols apparently reflects the restricted substrate

binding pocket. Enlarging the substrate binding pocket in *Sce*ADH1 with the T45S and W92A substitutions produced enzymes that were more active on branched chain and benzyl alcohols as compared to wild-type *Sce*ADH1, and the double substitution inverted the relative specificity for ethanol as compared to hexanol by a factor of 5000 [4]. The horse enzyme has Ser-48, Phe-93 and Val-294 corresponding to Thr-45, Trp-92 and Met/Leu-270 in yeast ADH. It remains to be determined why *Sce*ADH1 is twice as active as horse ADH on ethanol, whereas horse ADH is 24,000 times more active than SceADH1 on benzyl alcohol.

4.2. Transition State Analysis

Klinman previously studied structure-activity relationships with commercial yeast ADH [12, 14]. The major observations were a substantial electronic effect on the turnover for benzaldehyde reduction (ρ value of 2.1 against σ^+ for V_2/E_t), no electronic effect on turnover for benzyl alcohol oxidation, a modest electronic effect on benzaldehyde binding (ρ value of −0.9 for $1/K_p$), and a ρ value of 1.5 on the equilibrium constant for aldehyde reduction. The hydride transfer steps were predominantly rate-limiting as the average kinetic isotope effects (using NADD or NADH) were 3.6 on V_2/E_t (k_{cat}) for aldehyde reduction and 4.0 on V_1/E_t for oxidation of dideutero alcohols. The isotope effects could also be analyzed to show that the Michaelis constants for aldehyde or alcohol approximate the dissociation constants. Because the electronic effects on V_2/E_t were offset by the effects on binding of aldehyde so that the net value of ρ of 1.2 calculated for V_2/K_p was similar to the effect on the equilibrium constant, it was concluded that the electronic effects are on the ground state, rather than on the transition state. The lack of an electronic effect on benzyl alcohol oxidation then led to the conclusion "that there is little or no development of charge at C-7 at the transition state relative to the alcohol in the ground state" [14]. The implication that the transition state resembles the alcohol is puzzling because subsequent studies on the secondary isotope effects suggested that bond hybridization at the transition state resembles the aldehyde [15,42]. However, the interpretation of the isotope effects is complicated by the fact that hydride transfer occurs with quantum mechanical tunneling [16,43], and interpretation of secondary isotope effects can be affected by a lack of synchrony in rehybridization of the donor and acceptor carbons [44].

Structure-activity relationships were also studied with horse liver ADH for which benzyl alcohols and benzaldehydes are excellent substrates [45]. However, hydride transfer is not rate-limiting for steady-state reactions with wild-type enzyme, and a chemically activated form of liver ADH, for which hydride transfer is at least partially limiting, was used. Significant substituent effects were found with four *p*-substituted benzaldehydes, with a ρ value of 1.1 on V_2/E_t and an average deuterium kinetic isotope effect of 2.3, and a ρ value of about 0.6 on V_2/K_p. The reaction of three *p*-substituted benzyl alcohols showed only small substituent effects on V_1/E_t, but a ρ value of −0.6 can be estimated for the effects on V_1/K_b. These results are qualitatively similar to those with yeast ADH.

The interpretation of the results from the studies with the *p*-substituted aromatic substrates is complicated because of the involvement of the catalytic zinc that binds the oxygen of the substrate and the histidine that participates in acid/base catalysis through a hydrogen bond relay system. The enzyme can modulate the development of charge in the transition state. By analogy with the homologous horse liver ADH, we can suggest that the alcohol binds to the catalytic zinc, becomes deprotonated by the catalytic histidine, and is stabilized as the alkoxide by a low barrier hydrogen bond to the hydroxyl group of Thr-45 [39,46,47]. Rapid reaction kinetics suggest that the zinc-OH_2 loses a proton to form zinc-OH^- before alcohol displaces the water [48]. Subsequently, the hydride ion is transferred from the alkoxide to the oxidized nicotinamide ring and the zinc-bound aldehyde is formed. The inverse solvent isotope effects for the hydride transfer step (2-fold faster in D_2O than H_2O) with ethanol or benzyl alcohol and a proton inventory study with ethanol suggest that the transition state has a charge on the

oxygen of −0.3 [40,46]. Thus, the transition state may more closely resemble aldehyde than alcoholate, with respect to the charge on the oxygen, but the charge at C-7 in the transition state may be different.

The new results for reactions of *p*-substituted substrates with *Sce*ADH2 are qualitatively similar to the previous ones, but differ somewhat in the magnitudes of the effects and are more simply interpreted. The new results show that there are good linear correlations for both V_2/E_t and V_2/K_p with σ^+, producing ρ values of 1.9 and 1.7 with *p*-substituted benzaldehydes, respectively (Fig 2). In contrast to the previous results [12], it appears that there is no significant effect of the *p*-substituents on binding of the benzaldehydes. Note that V_2/K_p describes the bimolecular reaction of the enzyme-NADH complex with benzaldehyde to form the enzyme-NAD^+ complex and free benzyl alcohol, whereas V_2/E_t describes the conversion of the ternary enzyme-NADH-benzaldehyde complex to form free enzyme, NAD^+ and benzyl alcohol. When hydride transfer is the rate-limiting step and the kinetic mechanism is rapid equilibrium random [12,14], the difference in the ρ values for V_2/K_p and V_2/E_t would correspond to the ρ value for the binding of aldehyde. However, fitting of $\log(1/K_p)$ against σ^+ gave a ρ value of -0.2 ± 0.2, not a statistically significant fit. The ρ values of 1.7–1.9 appear to be larger than the ρ value of 1.5 for the equilibrium constant, which would be consistent with a substituent effect on the transition state. This would imply that the transition state develops some negative charge relative to aldehyde (as the hydride ion attacks), which is stabilized by electron withdrawing groups (promoting the reduction). The ρ values of 2.3–2.6 for reactions of benzaldehydes with $NaBH_4$ and HCN also suggest development of some negative charge [12], but as noted above, enzyme catalysis may modulate the charge and have different ρ values.

For the oxidation of the benzyl alcohols, the substituents slightly, but not significantly, affect V_1/E_t and V_1/K_b, and there does not appear to be an effect on binding of the alcohol (slope of Hammet plot = -0.13 ± 0.38). In contrast, the previous results with yeast ADH found that binding of alcohol was favored by hydrophobic effects [14].

Because it appears that hydride transfer is the rate limiting step for alcohol oxidation or aldehyde reduction, and there are only small effects of the substituents on binding, we can simplify the analysis of the effects by considering only the V/K_m parameters, which report on the energetics of the conversion of free substrate to the transition state for the forward and reverse reactions: E-NAD^+ + alcohol == E-NADH + aldehyde. This reaction is described by a rearranged Haldane equation: $K_{eq}K_{ia}/K_{iq} = (V_1/K_b)/(V_2/K_p)$. This relationship requires that $\rho(K_{eq}) = \rho(V_1/K_b) - \rho(V_2/K_p)$, and the present results fit within experimental error: ($-1.5 \approx 0.1 - 1.7$), when the reaction is written for alcohol oxidation. The conclusion from this analysis is that the major effect of the substituents is due to the free energies of the ground states of the substrates rather than the transition state energies. Electron withdrawing substituents promote aldehyde reduction because they favor the thermodynamics of the reaction. The activation energies for alcohol oxidation may be slightly affected by the *p*-substituents, whereas the activation energies for aldehyde reduction are significantly affected by the substitutents. The structure-activity studies do not fully define the transition state, but the lack of significant substituent effects on alcohol oxidation is consistent with a transition state that electronically resembles alcohol. Further studies of isotope effects and a comprehensive analysis of the tunneling are required.

The structure-activity results with *Sce*ADH2 are consistent with the previous studies with commercial ADH, and the same general interpretation applies, but how can we account for the quantitative differences between the previous and present studies? Different enzyme preparations were used, and it is possible that the commercial enzyme was a mixture of isoenzymes, although the ADH2 in that preparation might have contributed most of the activity. Different buffers and pH values were used, and the lower pH used in this study would facilitate

the reduction of aldehydes by promoting protonation of the alcoholate. Experimental errors giving a 2-fold difference on kinetic constants would yield differences of 0.3 on log plots, which is similar to the average differences between fitted and experimental values in Figs. 1 and 2. In order to increase the confidence in the kinetic analyses in this study, the range of compounds was extended to the -CN and -CF_3 compounds, which are much more electron-withdrawing. Using a narrower range of compounds gives different ρ values. It is also possible that hydride transfer is not completely rate limiting for all substrates with *Sce*ADH2, but the extremely low turnover numbers and catalytic efficiencies compared to good substrates is most consistent with a rapid equilibrium random mechanism. Despite the differences in the studies, it is gratifying that the major features of the structure-activity relationships are the same for the yeast ADHs.

Acknowledgments

This work was supported by NIH Grants AA06223 and GM078446 and NSF Grant MCB 91-18657. We thank Drs. Axel J. Ganzhorn, David W. Green, and Jeffrey S. Kavanaugh for preliminary observations that led to this work and Mark D. Hermes for some results. We thank Kristine B. Berst and The University of Iowa Macromolecular Structure Facility for the mass spectral analysis of the peptides from *Scb*ADH1. We thank Dr. Amnon Kohen for helpful discussions. We thank Drs. E. T. Young and B. D. Hall for the host yeast strains and the plasmids containing the genes for *Sce*ADH1 and *Sce*ADH2.

Abbreviations

ADH
: alcohol dehydrogenase

***Sce*ADH1**
: ADH I from *Saccharomyces cerevisiae*

***Sce*ADH2 and *Sce*ADH3**
: ADH isoenzymes II and III from *S. cerevisiae*

***Scb*ADH1**
: ADH I from *Saccharomyces carlsbergensis*

comADH
: commercial yeast ADH

V_1/E_t
: turnover number for alcohol oxidation

V_1/K_b
: V_1/E_tK_b, catalytic efficiency for alcohol oxidation

V_2/E_t **and** V_2/K_p
: V_2/E_tK_p, turnover number and catalytic efficiency for aldehyde reduction

References

1. Sund H, Theorell H. Alcohol Dehydrogenases. The Enzymes 1963;7:25–83.
2. Brändén CI, Jörnvall H, Eklund H, Furugren B. Alcohol Dehydrogenases. The Enzymes, 3rd Ed 1975;11:103–190.
3. Sun HW, Plapp BV. Progressive sequence alignment and molecular evolution of the Zn-containing alcohol dehydrogenase family. J Mol Evol 1992;34:522–535. [PubMed: 1593644]
4. Green DW, Sun HW, Plapp BV. Inversion of the substrate specificity of yeast alcohol dehydrogenase. J Biol Chem 1993;268:7792–7798. [PubMed: 8463307]

5. Dickinson FM, Dalziel K. The specificities and configurations of ternary complexes of yeast and liver alcohol dehydrogenases. Biochem J 1967;104:165–172. [PubMed: 4291993]
6. Jörnvall H. The primary structure of yeast alcohol dehydrogenase. Eur J Biochem 1977;72:425–442. [PubMed: 320000]
7. Young, T.; Williamson, V.; Taguchi, A.; Smith, M.; Sledziewski, A.; Russell, D.; Osterman, J.; Denis, C.; Cox, D.; Beier, D. The alcohol dehydrogenase genes of the yeast, *Saccharomyces cerevisiae*: isolation, structure, and regulation. In: Hollaender, A.; DeMoss, RD.; Kaplan, S.; Konisky, J.; Savage, D.; Wolfe, RS., editors. Genetic Engineering of Microorganisms for Chemicals. Plenum Publishing; New York: 1982. p. 335-361.
8. Bennetzen JL, Hall BD. The primary structure of the *Saccharomyces cerevisiae* gene for alcohol dehydrogenase. J Biol Chem 1982;257:3018–3025. [PubMed: 6277922]
9. Russell DW, Smith M, Williamson VM, Young ET. Nucleotide sequence of the yeast alcohol dehydrogenase II gene. J Biol Chem 1983;258:2674–2682. [PubMed: 6337160]
10. Young ET, Pilgrim D. Isolation and DNA sequence of *ADH3*, a nuclear gene encoding the mitochondrial isozyme of alcohol dehydrogenase in *Saccharomyces cerevisiae*. Mol Cell Biol 1985;5:3024–3034. [PubMed: 2943982]
11. Ganzhorn AJ, Green DW, Hershey AD, Gould RM, Plapp BV. Kinetic characterization of yeast alcohol dehydrogenases. Amino acid residue 294 and substrate specificity. J Biol Chem 1987;262:3754–3761. [PubMed: 3546317]
12. Klinman JP. The mechanism of enzyme-catalyzed reduced nicotinamide adenine dinucleotide-dependent reductions. Substituent and isotope effects in the yeast alcohol dehydrogenase reaction. J Biol Chem 1972;247:7977–7987. [PubMed: 4344986]
13. Klinman JP. Acid-base catalysis in the yeast alcohol dehydrogenase reaction. J Biol Chem 1975;250:2569–2573. [PubMed: 235517]
14. Klinman JP. Isotope effects and structure-reactivity correlations in the yeast alcohol dehydrogenase reaction. A study of the enzyme-catalyzed oxidation of aromatic alcohols. Biochemistry 1976;15:2018–2026. [PubMed: 773429]
15. Welsh KM, Creighton DJ, Klinman JP. Transition-state structure in the yeast alcohol dehydrogenase reaction: the magnitude of solvent and alpha-secondary hydrogen isotope effects. Biochemistry 1980;19:2005–2016. [PubMed: 6990968]
16. Cha Y, Murray CJ, Klinman JP. Hydrogen tunneling in enzyme reactions. Science 1989;243:1325–1330. [PubMed: 2646716]
17. Wills C, Jörnvall H. The two major isozymes of yeast alcohol dehydrogenase. Eur J Biochem 1979;99:323–331. [PubMed: 387413]
18. Rainbow, C. Brewer's Yeast. In: Rose, AH.; Harrison, JS., editors. The Yeasts. Academic Press; New York: 1970. p. 148
19. Hammond, JR. The Yeasts. Academic Press; New York: 1993. Brewer's Yeast; p. 7-67.
20. Børsting C, Hummel R, Schultz ER, Rose TM, Pedersen MB, Knudsen J, Kristiansen K. *Saccharomyces carlsbergensis* contains two functional genes encoding the Acyl-CoA binding protein, One similar to the *ACB1* gene from *S. cerevisiae* and one identical to the *ACB1* gene from *S. monacensis*. Yeast 1997;13:1409–1421. [PubMed: 9434347]
21. Dunn B, Sherlock G. Reconstruction of the genome origins and evolution of the hybrid lager yeast *Saccharomyces pastorianus*. Genome Res 2008;18:1610–1623. [PubMed: 18787083]
22. Sherman, F.; Fink, GR.; Hicks, JB. Laboratory Course Manual for Methods in Yeast Genetics. Cold Spring Harbor Laboratory; Cold Spring Harbor, New York: 1986.
23. Sambrook, J.; Fritsch, EF.; Maniatis, T. Molecular Cloning: A Laboratory Manual. Vol. 2. Cold Spring Harbor Laboratory; Cold Spring Harbor, New York: 1989.
24. Sanger F, Nicklen S, Coulson AR. DNA sequencing with chain-terminating inhibitors. Proc Natl Acad Sci U S A 1977;74:5463–5467. [PubMed: 271968]
25. Gould RM, Plapp BV. Substitution of arginine for histidine-47 in the coenzyme binding site of yeast alcohol dehydrogenase I. Biochemistry 1990;29:5463–5468. [PubMed: 2201405]
26. Laemmli UK. Cleavage of structural proteins during the assembly of the head of bacteriophage T4. Nature 1970;227:680–685. [PubMed: 5432063]

27. Theorell H, Yonetani T. Liver alcohol dehydrogenase-DPN-pyrazole complex: A model of a ternary intermediate in the enzyme reaction. Biochem Z 1963;338:537–553. [PubMed: 14087322]
28. Cleland WW. Statistical analysis of enzyme kinetic data. Methods Enzymol 1979;63:103–138. [PubMed: 502857]
29. Shearer GL, Kim K, Lee KM, Wang CK, Plapp BV. Alternative pathways and reactions of benzyl alcohol and benzaldehyde with horse liver alcohol dehydrogenase. Biochemistry 1993;32:11186–11194. [PubMed: 8218182]
30. Ganzhorn AJ, Plapp BV. Carboxyl groups near the active site zinc contribute to catalysis in yeast alcohol dehydrogenase. J Biol Chem 1988;263:5446–5454. [PubMed: 3281940]
31. Fan F, Lorenzen JA, Plapp BV. An aspartate residue in yeast alcohol dehydrogenase I determines the specificity for coenzyme. Biochemistry 1991;30:6397–6401. [PubMed: 2054345]
32. Wratten CC, Cleland WW. Product inhibition studies on yeast and liver alcohol dehydrogenases. Biochemistry 1963;2:935–941. [PubMed: 14087384]
33. Dickinson FM, Monger GP. A study of the kinetics and mechanism of yeast alcohol dehydrogenase with a variety of substrates. Biochem J 1973;131:261–270. [PubMed: 4352908]
34. Dickenson CJ, Dickinson FM. A study of the oxidation of butan-1-ol and propan-2-ol by nicotinamide-adenine dinucleotide catalysed by yeast alcohol dehydrogenase. Biochem J 1975;147:541–547. [PubMed: 170911]
35. Cook PF, Cleland WW. pH variation of isotope effects in enzyme-catalyzed reactions. 1. Isotope- and pH-dependent steps the same. Biochemistry 1981;20:1797–1805. [PubMed: 7013800]
36. Dickinson FM, Dalziel K. Substrate specificity and stereospecificity of alcohol dehydrogenases. Nature 1967;214:31–33. [PubMed: 4292416]
37. Hammett, LP. Physical Organic Chemistry. McGraw-Hill; New York: 1970.
38. Hansch, C.; Leo, A. Substituent Constants for Correlation Analysis in Chemistry and Biology. Wiley; New York: 1979. p. 1-63.
39. Ramaswamy S, Eklund H, Plapp BV. Structures of horse liver alcohol dehydrogenase complexed with NAD^+ and substituted benzyl alcohols. Biochemistry 1994;33:5230–5237. [PubMed: 8172897]
40. Sekhar VC, Plapp BV. Rate constants for a mechanism including intermediates in the interconversion of ternary complexes by horse liver alcohol dehydrogenase. Biochemistry 1990;29:4289–4295. [PubMed: 2161681]
41. Lee KM, Dahlhauser KF, Plapp BV. Reactivity of horse liver alcohol dehydrogenase with 3-methylcyclohexanols. Biochemistry 1988;27:3528–3532. [PubMed: 3390450]
42. Klinman JP. Probes of mechanism and transition-state structure in the alcohol dehydrogenase reaction. CRC Crit Rev Biochem 1981;10:39–78. [PubMed: 7011676]
43. Nagel ZD, Klinman JP. Tunneling and dynamics in enzymatic hydride transfer. Chem Rev 2006;106:3095–3118. [PubMed: 16895320]
44. Pu J, Ma S, Garcia-Viloca M, Gao J, Truhlar DG, Kohen A. Nonperfect synchronization of reaction center rehybridization in the transition state of the hydride transfer catalyzed by dihydrofolate reductase. J Am Chem Soc 2005;127:14879–14886. [PubMed: 16231943]
45. Dworschack RT, Plapp BV. pH, isotope, and substituent effects on the interconversion of aromatic substrates catalyzed by hydroxybutyrimidylated liver alcohol dehydrogenase. Biochemistry 1977;16:2716–2725. [PubMed: 19037]
46. Ramaswamy S, Park DH, Plapp BV. Substitutions in a flexible loop of horse liver alcohol dehydrogenase hinder the conformational change and unmask hydrogen transfer. Biochemistry 1999;38:13951–13959. [PubMed: 10529241]
47. Plapp, BV. Catalysis by Alcohol Dehydrogenases. In: Kohen, A.; Limbach, H-H., editors. Isotope Effects in Chemistry and Biology. CRC Press, Taylor and Francis; Boca Raton: 2006. p. 811-835.
48. Kovaleva EG, Plapp BV. Deprotonation of the horse liver alcohol dehydrogenase-NAD^+ complex controls formation of the ternary complexes. Biochemistry 2005;44:12797–12808. [PubMed: 16171395]
49. Plapp BV. Enhancement of the activity of horse liver alcohol dehydrogenase by modification of amino groups at the active sites. J Biol Chem 1970;245:1727–1735. [PubMed: 4314596]

50. Bäcklin KI. The equilibrium constant of the system ethanol, aldehyde, DPN+, DPNH and H+ Acta Chem Scand 1958;12:1279–1285.

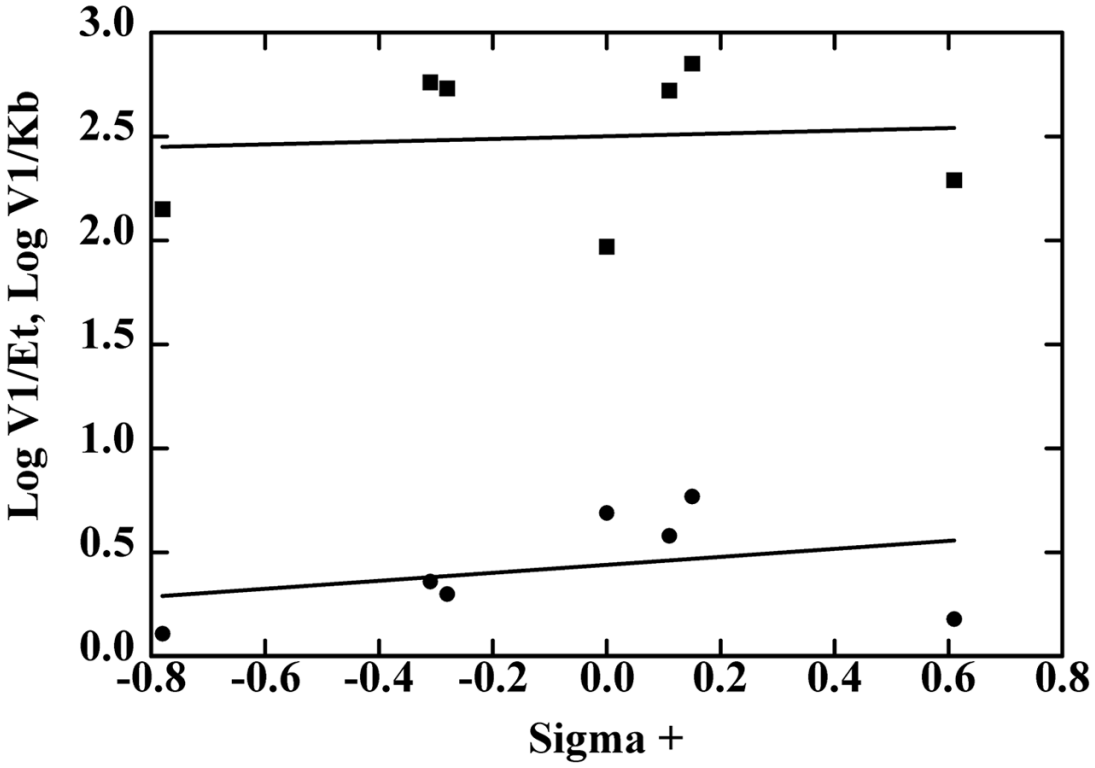

Fig. 1.

Hammett plots of the quantitative structure-activity relationship for oxidation of *p*-substituted benzyl alcohols by *Sce*ADH2. The data are from Table 6, where V_1/E_t (●) and V_1/K_b (■) are plotted against the σ^+ values for CH_3O-, CH_3- $CH(CH_3)_2$- H-, Cl-, Br-CF_3-, from left to right. The lines were calculated by linear regression, but the slopes were not significantly determined: for log (V_1/E_t) slope is (0.19 ± 0.25)σ^+, and for log (V_1/K_b) slope is (0.06 ± 0.36)σ^+.

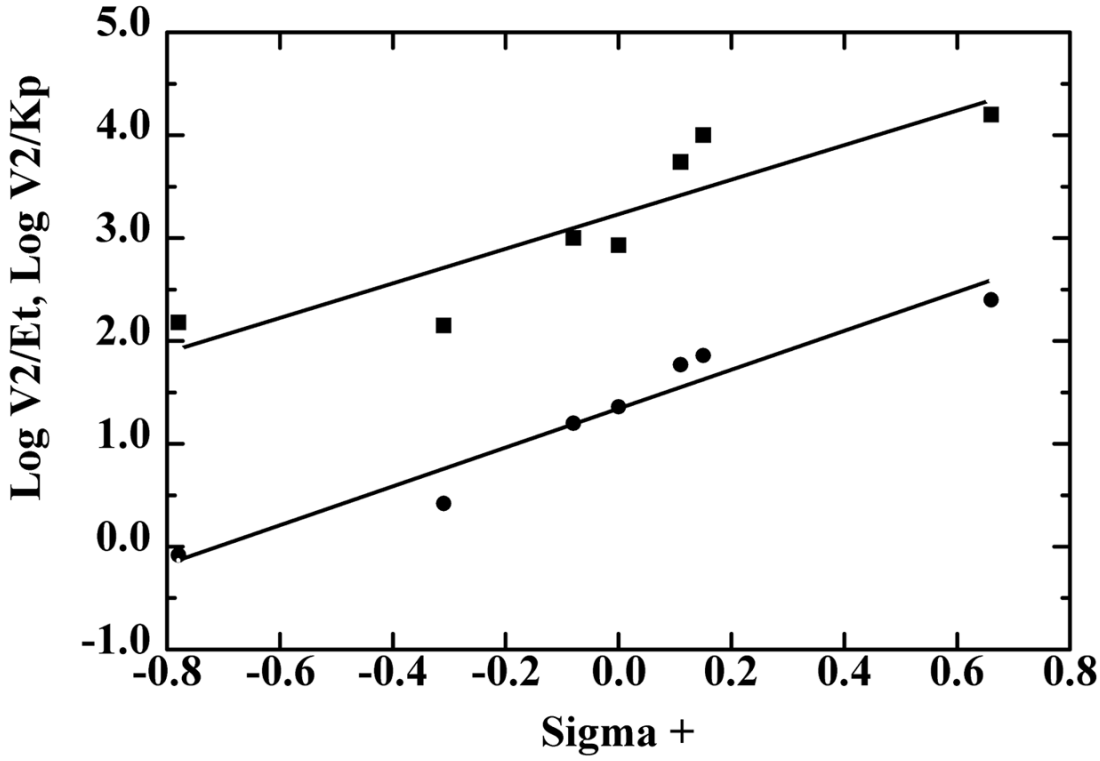

Fig. 2.

Hammett plots of the quantitative structure-activity relationship for reduction of *p*-substituted benzaldehydes by *Sce*ADH2. The data are from Table 7, where V_2/E_t (●) and V_2/K_p (■) are plotted against the σ^+ values for CH_3O-, CH_3-, H-, Cl-, Br- CN-, from left to right. and lines were calculated by linear regression with the following results.

$$\text{Log}\,(V_2/E_t)=(1.89 \pm 0.21)\sigma^{+}+(1.34 \pm 0.087),\text{F}=80.3,\text{R}^2=0.94$$

$$\text{Log}\,(V_2/K_p)=(1.68 \pm 0.39)\sigma^{+}+(3.22 \pm 0.16),\text{F}=18.4,\text{R}^2=0.79$$

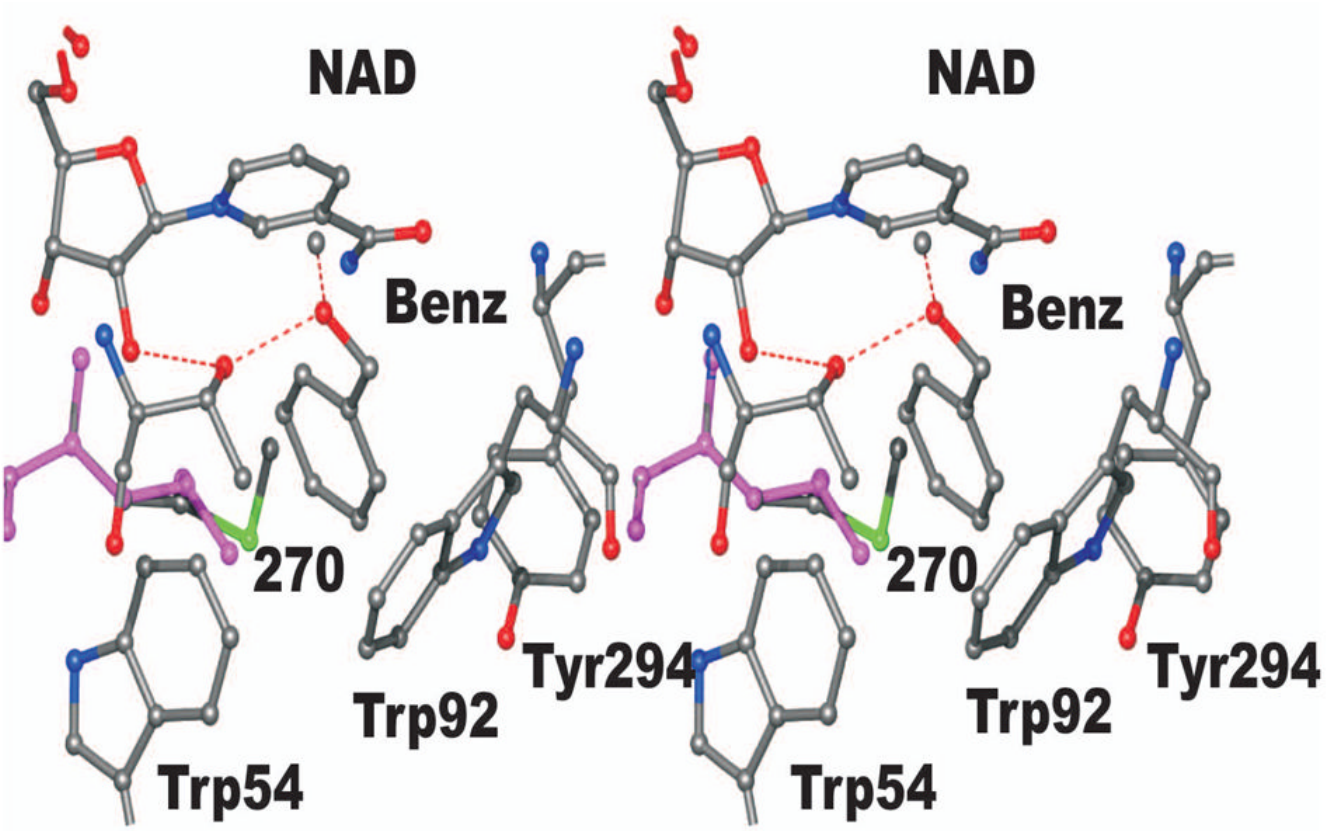

Fig. 3.

Model of the active site of yeast alcohol dehydrogenase with benzyl alcohol bound. The coordinates are based on the structure of the *Sce*ADH1 complexed with NAD^+ and 2,2,2-trifluoroethanol (2HCY.pdb), with benzyl alcohol replacing trifluoroethanol. In this model, the oxygen of benzyl alcohol binds the catalytic zinc and the hydroxyl group of Thr-45. The benzene ring makes some unfavorable steric contacts with the three labeled aromatic amino acid residues and especially with Met-270. By substituting Met-270 with Leu-270 (which has the compact isopropyl group) these bad contacts are relieved, but the other close contacts remain.

Table 1

Comparison of Amino Acid Sequences of Yeast Alcohol Dehydrogenases

Residue no.	***Sce*ADH1**	***Scb*ADH1**	***com*ADH**	***Sce*ADH2**	***Sce*ADH3**
58	Val	Thr	Thr	Thr	Val
127	Gln	Glu	Glu[a]	Glu	Gln
147	Gln	Glu	Glu	Glu	Glu
151	Ile	Val	Val	Ile	Ile

Residues that differ between *Sce*ADH1 [8] and *Scb*ADH1 are listed, as well as the comparable residues for commercial enzyme [6], *Sce*ADH2 [9] and for *Sce*ADH3 [10].

[a] Jörnvall [6] determined Gln, but we determined Glu by analysis of peptides by LC/MS (not shown).

Table 2

Relative Electrophoretic Mobilities of the Yeast Alcohol Dehydrogenases

***Sce*ADH1**	***Scb*ADH**	***Sce*ADH2**	***Sce*ADH3**
0.29	0.45	0.50	0.09

The R_f values are calculated relative to the dye front in electrophoresis in 6% polyacrylamide gel under non-denaturing conditions [26].

Table 3

Kinetic Constants for Yeast Alcohol Dehydrogenases

Kinetic constant[a]	*Sce*ADH1[b]	*Scb*ADH1	*Sce*ADH2[c]
K_a (μM)	160	190	110
K_b (μM)	21,000	18,000	810
K_p (μM)	740	1080	90
K_q (μM)	94	210	50
K_{ia} (μM)	950	1300	580
K_{iq} (μM)	31	50	11
V_1/E_t (s^{-1})	360	480	130
V_2/E_t (s^{-1})	1800	3500	1000
Activity (s^{-1})[d]	400	500	220
*K*eq (pM)[e]	12	16	12

[a] Activity was measured at 30 °C in 83 mM potasium phosphate buffer, pH 7.3, containing 40 mM KCl, and 0.25 mM EDTA. K_a, K_b, K_p and K_q are the Michaelis constants for NAD^+, ethanol, acetaldehyde and NADH, respectively; K_i values are the inhibition constants, and V_1/E_t and V_2/E_t are the turnover numbers for ethanol oxidation and acetaldehyde reduction. The kinetic constants for *Sce*ADH2 were determined from product inhibition studies. The errors were less than 15 % of the values.

[b] Data from [25].

[c] Data from [11].

[d] The turnover number in the standard assay [49] is based on titration of active sites.

[e] The equilibrium constants calculated using the Haldane equation, $K_{eq} = (V_1 K_p K_{iq}[H^+])/(V_2 K_b K_{ia})$, are similar to the established value of 12 pM at 30 °C [50].

Table 4

Survey of Activities on Branched and Long Chain Aliphatic Alcohols[a]

Enzyme	2-Propanol	*R*-2- Butanol	*S*-2- Butanol	2-Methyl-1-propanol	*S*-2- Methyl-1-butanol	*R,S*-2- Methyl-1-butanol	3- Methyl-1-butanol	Pentanol	Octanol
					V_1/E_t (s^{-1})				
*Sce*ADH1	4.1	0.026	0.92	0.022	0.0018	0.0036	0.042	6.0	2.5
*Scrl*ADH	5.1	0.030	1.2	0.026	0.003	0.02	0.046	9.1	9.3
*Sce*ADH2	23	0.44	13	0.70	0.20	0.11	0.042	93	51
					K_b (mM)				
*Sce*ADH1	150	59	55	41	14	24	29	24	2.1
*Scrl*ADH	110	53	43	31	13	60	46	40	5.2
*Sce*ADH2	130	110	96	55	28	21	26	7.5	0.50
					V_1/K_b ($M^{-1}s^{-1}$)				
*Sce*ADHI	27	0.48	14	0.54	0.13	0.14	0.14	250	1200
*Scrl*ADH	28	0.58	28	0.84	0.22	0.42	1.0	230	1800
*Sce*ADH2	180	4.0	140	13	0.71	5.2	16	12000	100000
					Highest alcohol concentrations (mM)				
*Sce*ADHI	500	200	100	100	100	100	100	70	1.6
*Scrl*ADH	500	200	100	100	100	100	100	70	1.6
*Sce*ADH2	300	200	50	100	100	200	100	70	1.6

[a] The NAD^+ concentration was fixed at 1 mM, and substrate concentrations were varied over a 5-fold range of K_b with the highest concentrations used indicated in the table. The kinetic constants are apparent because the concentration of NAD^+ was not saturating.

Table 5

Survey of Activities on Benzyl Alcohols and Benzaldehydes[a]

Enzyme	Benzyl alcohol	*p*-Methoxy- benzyl alcohol	Benzaldehyde	*p*-Methoxy- benzaldehyde
		V/E_t (s^{-1})		
*Sce*ADH1	0.012	0.058	0.91	0.075
*Scb*ADH1	0.011	0.11	0.52	0.071
*Sce*ADH2	1.9	0.87	12	0.86
		K_m (mM)		
*Sce*ADH1	34	11	33	2.9
*Scb*ADH1	24	22	23	3.4
*Sce*ADH2	49	6.9	14	5.9
		V/K_m ($M^{-1}s^{-}1$)		
*Sce*ADH1	0.32	5.3	27	26
*Scb*ADH1	0.48	4.5	23	21
*Sce*ADH2	38	130	860	150
		Highest Concentrations of Alcohols and Aldehydes (mM)		
*Sce*ADH1	25	15	32	5
*Scb*ADH1	25	15	32	5
*Sce*ADH2	25	35	55	5

[a] Assays used 2 mM NAD^+ and different concentrations of NADH (250 μM NADH for benzaldehyde and 100 μM NADH for *p*-methoxybenzaldehyde). V is V_1 for alcohols and V_2 for aldehydes. K_m is the K_b for the alcohols and K_p for the aldehydes. The kinetic constants are apparent because the concentrations of coenzymes were not saturating.

Table 6

Kinetic Constants for the Oxidation of *p*-Substituted Benzyl Alcohols by *Sce*ADH2[a]

Alcohols	K_a (mM)	K_b (mM)	K_{ia} (mM)	V_1/E_t (s^{-1})	V_1/K_b ($M^{-1}s^{-1}$)
CH_3O-	1.0	9.4	0.20	1.3	140
CH_3-	0.66	4.1	1.20	2.3	570
$CH(CH_3)_2$-	1.2	3.6	0.56	2.0	540
H-	7.5	16	3.6	1.5	94
Cl-	1.2	7.2	0.42	3.8	530
Br-	1.3	8.4	0.37	5.9	700
CF_3-	4.2	7.7	2.3	1.5	190

[a]Data were fitted with SEQUEN program to the equation $v = VAB/(K_{ia}K_b + K_aB + K_bA + AB)$, where A and B are substrate concentrations; K_a and K_b are the Michaelis constants for NAD^+ and ethanol; K_{ia} is the inhibition constant for NAD^+; V_1/E_t is the turnover number and V_1/K_b ($= V_1/E_tK_b$) is the catalytic efficiency for alcohol oxidation.

Table 7

Kinetic Constants for Reduction of *p*-Substituted Benzaldehydes by *Sce*ADH2[a]

Aldehyde	K_q (μM)	K_p (mM)	K_{iq} (μM)	V_2/E_t (s^{-1})	V_2/K_p ($M^{-1}s^{-1}$)
CH_3O-	17	5.5	5.6	0.83	150
CH_3-	89	19	1.7	2.6	140
F-	24	17	11	16	930
H-	240	26	*b*	23	860
Cl-	84	11	20	59	5400
Br-	11	7.2	12	73	10000
CN-	400	16	6.7	250	15000

[a]Data were fitted with the SEQUEN program. K_q and K_p are the Michaelis constants for NADH and acetaldehyde. K_{iq} is the inhibition constant for NADH. V_2/E_t is the turnover number and V_2/K_p is the catalytic efficiency for aldehyde reduction.

[b]Value not determined as the data fit best to the equation for a Ping Pong mechanism, where $K_{iq} = 0$.